Copper Substrate Dissolution in Eutectic Sn-Ag Solder and Its Effect on Microstructure

S. CHADA,[1,2] R.A. FOURNELLE,[1] W. LAUB,[1,3] and D. SHANGGUAN[4]

1.—Marquette University, Materials Science and Engineering Program, Milwaukee, WI 53201. 2.—Presently at Motorola, 8000 West Sunrise Blvd., Fort Lauderdale, FL 33322. 3.—Presently at Solectron GmbH, Solectronstr. 2, 71083 Herrenberg, Germany. 4.—Ford Motor Company, Visteon Automotive Systems, 17000 Rotunda Drive, Dearborn, MI 48121

The dissolution of Cu into molten Sn-3.8at.%Ag (Sn-3.5wt.%Ag) solder and its effect on microstructure were studied by light microscopy, scanning microscopy, and x-ray microanalysis. X-ray microanalysis of the average Cu content of samples soldered under various conditions showed that the amount of Cu dissolved during soldering increased with increasing soldering temperature and time and that the rate of dissolution could be described by a Nernst-Brunner equation. Microstructurally it was found that the volume fractions of primary β(Sn) dendrites and η-phase dendrites increase with increasing soldering temperature and time. The microstructural changes can be explained using Sn-Ag-Cu phase equilibrium data. A numerical method was developed for calculating the amount of Cu dissolved under non-isothermal conditions, which describes dissolution reasonably well.

Key words: Eutectic Sn-Ag solder, Cu substrate, dissolution

INTRODUCTION

It is well known that soldering involves a reaction between molten solder and substrate, which forms some sort of intermetallic layer and which dissolves some of the substrate[1]. In soldering on Cu substrates with Sn based solders such as Sn-3.8at.%Ag it is well known that the reaction involves the formation of an intermetallic layer consisting of ε(Cu_3Sn) and η(Cu_6Sn_5) and the dissolution of some of the Cu substrate, enriching the molten solder with Cu.[1] Previous studies[2] have shown that the amount of dissolved Cu influences the rate at which the intermetallic forms. The present work examines how the dissolution of Cu by molten Sn-3.8at.%Ag solder affects the microstructure of the solder. A numerical method is also presented for predicting the amount of Cu dissolved under non-isothermal conditions. This method requires as input experimentally determined Nernst-Brunner parameters for isothermal dissolution as well as experimentally determined solubility limit data for the solubility of Cu in molten Sn-3.8at.%Ag solder.

(Received March 14, 2000; accepted July 7, 2000)

EXPERIMENTAL PROCEDURE

Materials and Soldering Procedures

Solder paste containing Sn-3.8at.%Ag solder in a mildly activated rosin (RMA) flux as well as bulk solder of the same composition were used to prepare the various samples used. These materials were reflow soldered on 1 mm thick 99.9wt.%Cu sheet specimens of various sizes. All Cu sheet specimens were cleaned in a solution of equal parts by volume of nitric, acetic and phosphoric acids and then rinsed in water and methanol prior to soldering.

For studies of the microstructural changes in the Sn-3.8at.%Ag solder resulting from Cu dissolution in the molten solder under isothermal conditions at temperatures ranging from 500 K (226°C) to 565 K (292°C), 10 mm × 5 mm ×1 mm Cu substrates were first preheated to the desired reflow temperature on a Dataplate Series 730 programmable hot plate, with the temperature-time profile being monitored by a dummy Cu specimen that had a fine gage chromel-alumel thermocouple imbedded in an appropriate amount of solder on it. After the specimen had at-

tained the reflow temperature, a small amount of activated rosin (AR) flux was added to break up the oxide layer on the Cu surface. Then, after waiting an additional 30 sec for the temperature of the specimen to recover, a fixed amount of solder paste (≈0.1 g) was applied with an EFD 1000 DV-SMT dispenser. The resulting Cu area to solder volume ratio was approximately 3.7 mm^2/mm^3. The solder paste spread over the Cu substrate immediately, and melting occurred within a few seconds. The time at which melting occurred was taken as the start time for Cu dissolution. At times ranging from 20 sec to 8 min samples were removed from the hot plate and quenched on an iron block. The average cooling rate was measured to be on the order of 1500 K/min.

For studies of the isothermal dissolution of Cu in molten solder using a Nernst-Brunner analysis at 527 K (254°C), 545 K (272°C), and 575 K (302°C), 10 mm × 10 mm × 1 mm Cu substrates were reflow soldered as described above for times (t) of 60 sec, 120 sec, and 240 sec. However, instead of solder paste, 0.2 mm and 0.4 mm thick pieces of solder sheet 10 mm × 10 mm were used. This gave two different volumes of solder. After soldering, the substrate contact area (A) was measured and the solder volume (V) was determined by weighing the sample and subtracting the weight of the Cu substrate. Thus, for each temperature six different At/V values were available for determining the Nernst-Brunner parameter K, to be described later.

For determining the solubility limits of Cu in molten solder at temperatures ranging from 303 K (230°C) to 573 K (300°C), 10 mm × 10 mm × 1 mm Cu substrates were reflow soldered isothermally with 10 mm × 10 mm × 0.5 mm pieces of solder. The solder and substrate were coated with an RMA flux and then reflowed in either a VWR Scientific 1330 FM convection oven or a Lindberg muffle furnace for either 5 h or 10 h. Based on the Nernst-Brunner dissolution studies it was known that 5 h was sufficient to guarantee saturation of the solder with Cu. The actual reflow temperatures were measured with a thermocouple located near the specimens.

For the study of copper dissolution under non-isothermal conditions, six 10 mm × 5 mm × 1 mm Cu specimens were used. After cleaning the Cu substrates, approximately 0.1 g of solder paste was dispensed on them with an EFD 1000 DV-SMT dispenser. These specimens were then heated to peak reflow temperatures of either 513 K (244°C) or 535 K (262°C) at a rate of 5.6°/min on either a Dataplate Series 730 programmable hot plate or in a Despatch 924D forced convection oven equipped with a DRP-13 digital rate controller and using CO_2 as a coolant. The specimens were cooled from the peak reflow temperatures at rates ranging from 4.4°/min to 1210°/min. The faster cooling rates were attained by quenching on a Cu block from the hot plate, and the slower rates were attained by controlled cooling in the convection oven. All temperature-time profiles were followed with a fine gage chromel-alumel thermocouple in a dummy specimen and a strip chart recorder.

Metallography

Specimens for metallographic examination and x-ray microanalysis of average dissolved Cu content were sectioned perpendicular to the solder/substrate interface with a Buehler Isomet low speed saw with a high concentration diamond wafering blade. The cross sections for metallographic examination were then mounted in epoxy, ground through 1200 SiC paper and polished with 6 μm and 1 μm diamond paste on a Buehler Texmet polishing cloth. After cleaning ultrasonically in de-ionized water, final polishing was done using Buehler Mastermet colloidal silica solution on a Buehler Chemomet polishing cloth. The polished specimens were then rinsed in de-ionized water and methanol, dried, and etched in a solution of 2.5% HNO_3 and 1% HCl in methanol for 2 sec to 5 sec. The x-ray microanalysis specimens were just ground through 600 grit SiC.

Bright field light optical micrographs of solder microstructures were obtained at X1500 using a Bausch & Lomb Research Metallograph with an X85 oil immersion objective, with a stage micrometer being used to check the magnification. Measurements of the volume fraction of primary η phase dendrites, primary β(Sn) phase dendrites, and eutectic were made by point counting.

Microanalysis

The average Cu concentration in the solder of dissolution and solubility limit study specimens was determined by energy dispersive spectroscopy (EDS) with a NORAN Series II analyzer on a JEOL JSM 35 scanning electron microscope operated at 25 kV from specimens ground through 600 grit SiC. The background and ZAF corrected relative integrated intensity ratios of the Cu Kα, Sn Lα, and Ag Lα peaks were obtained from three areas on each specimen scanned at X50 for 200 sec using the NORAN SSQ program. The atomic percent Cu for each analysis was obtained from a calibration curve relating relative intensity ratios to Cu content. This curve was established using solder standards containing 0, 1, 2, 3, and 4 wt.%Cu.

RESULTS AND DISCUSSION

Isothermal Dissolution of Cu Substrate and Solubility of Cu in Molten Solder

Figures 1 and 2 show the results of EDS measurements of the average amount of Cu dissolved in molten solder at saturation (X_S) and under various conditions short of saturation (X), respectively. The solubility temperatures given in Fig. 1 are 50 K to 100 K below the reported liquidus temperatures for the η+liquid phase field in the binary Cu-Sn system.[3] This is expected in that, as described in the next section, 3.8at.%Ag will lower the equilibrium temperatures for the equilibrium between η and liquid. The data were fit with an Arrhenius equation of the form,

$$X^s = X^{SO} \exp(-Q_S/RT) \quad (1)$$

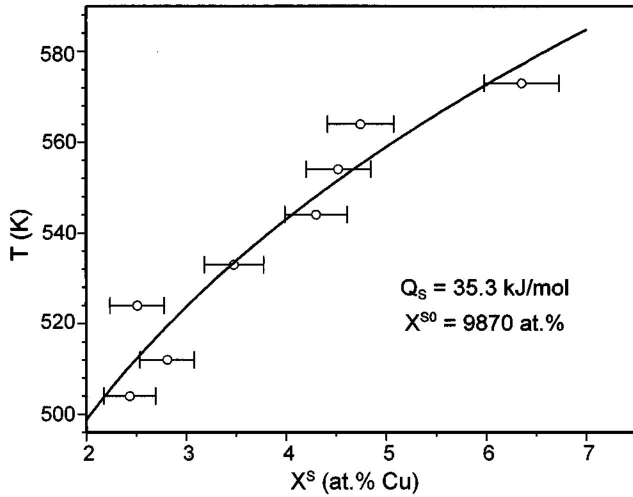

Fig. 1. Energy dispersive spectroscopy (EDS) measurements of the average Cu content in solder saturated with Cu at various temperatures. The Curve represents a fit of the data with the equation $X^S = X^{S0}\exp(-Q_S/RT)$.

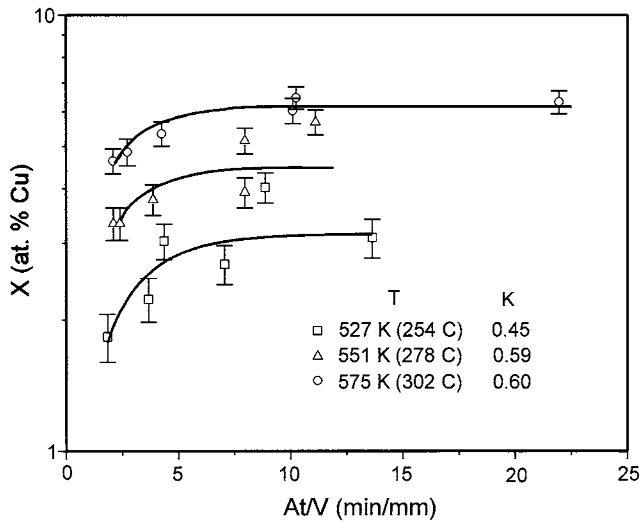

Fig. 2. Energy dispersive spectroscopy (EDS) measurements of the average Cu content of isothermally reflowed specimens having two different substrate surface area (A) to solder volume (V) ratios and reflowed for 60 sec, 120 sec, and 240 sec. The curves represent fits of the Nernst-Brunner equation (Eq. 2) to the data. The K values are those obtained from the curve fits.

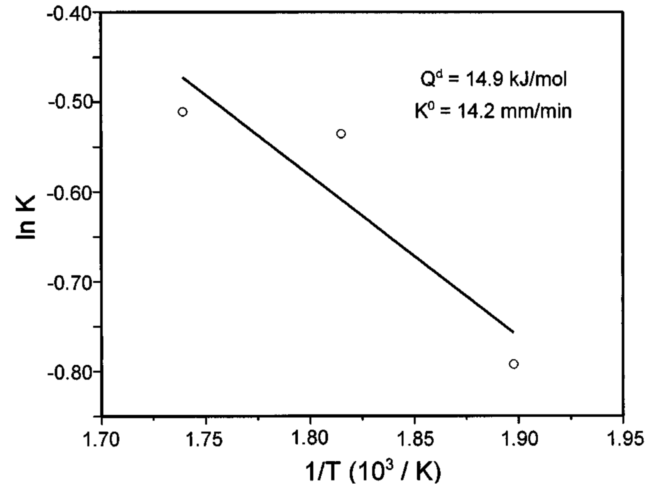

Fig. 3. Arrhenius plot of the Nernst-Brunner K values obtained from curve fits of the data in Fig. 2. The straight line represents a fit of the data with Eq. 3.

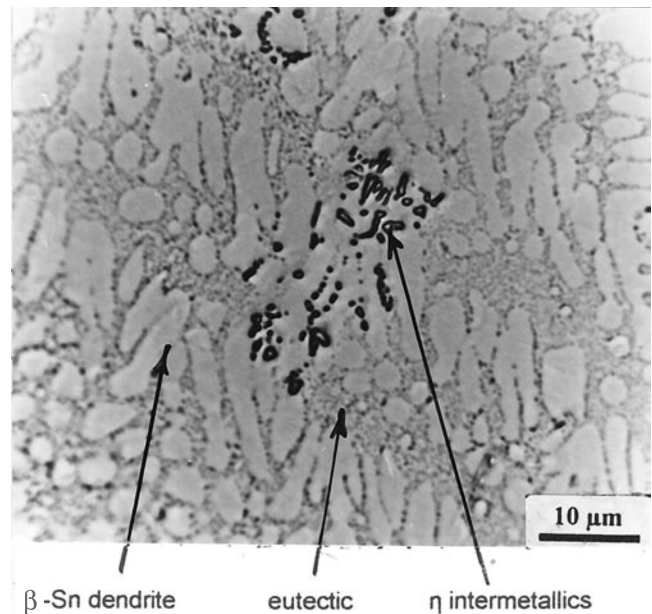

Fig. 4. Sample isothermally reflowed for 8 minutes at 499 K (226°C) showing β(Sn) dendrites, interdendritic eutectic mixture of Ag_3Sn in a β(Sn) matrix, and η-intermetallics.

to give the parameters Q_S = 35.3 kJ/mol and X_{SO} = 9870 at.% needed by the numerical method for predicting Cu dissolution under non-equilibrium conditions described in a later section.

The dissolution data in Fig. 2 show that the atomic percent (X) of dissolved Cu increases and then levels off with an increase in the Nernst-Brunner parameter At/V. These isothermal sets of data were fit with the Nernst-Brunner equation valid for constant atomic volume,

$$\ln \frac{X^S - X^O}{X^S - X} = \frac{KAt}{V} \qquad (2)$$

to obtain the curves in the figure. Here X_0 is the initial concentration of Cu in the molten solder. Values of X^S from the curve fit to the solubility data in Fig. 1 were used in making these curve fits. The curve fits in Fig. 2 yielded the values of K, the Nernst-Brunner dissolution rate constant, presented in the Arrhenius plot in Fig. 3. These three data points were, in turn, fit with a straight line of the form,

$$K = K^O \exp\left(-\frac{Q_d}{RT}\right) \qquad (3)$$

to yield the parameters Q_d and K^O needed by the numerical method for predicting the amount of Cu dissolution under non-isothermal conditions described in a later section.

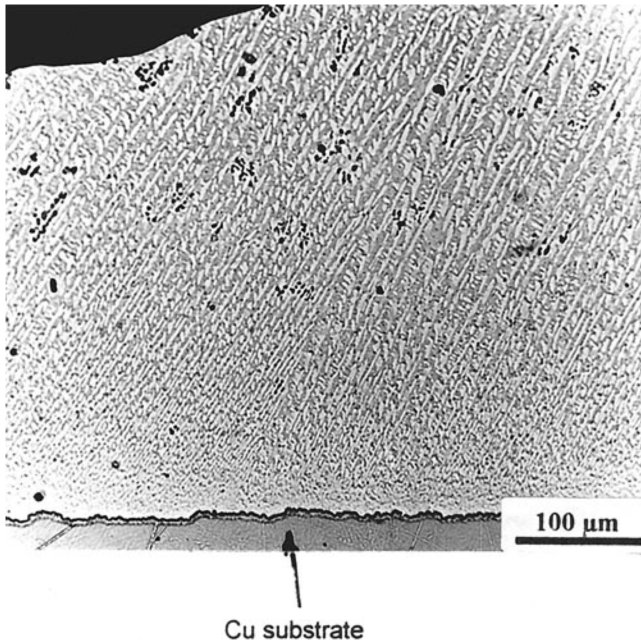

Fig. 5. Sample isothermally reflowed for 4 min at 499 K (226°C) showing inhomogeneity in the solder cross section.

Microstructural Changes in Solder Accompanying Cu Substrate Dissolution

Optical microscopy of solidified solder after isothermal dissolution of Cu substrate showed the following features: β(Sn) dendrites, an interdendritic eutectic mixture of Ag_3Sn in a β(Sn) matrix, and intermetallic dendrites (Fig. 4). X-ray microanalysis of the intermetallic dendrites present confirmed that they were η(Cu_6Sn_5) phase. Apparently sufficient Cu dissolved during reflow to result in the formation of η phase during solidification. Also, the solder cross section perpendicular to the solder/substrate interface presented in Fig. 5 shows that the microstructure of the solder on the substrate is inhomogeneous. As can be seen, the β(Sn)-dendrite size increases with increasing distance from the Cu substrate, as does the amount of η phase.

The micrographs in Fig. 6a–c of samples isothermally reflowed for 60 sec at temperatures of 509 K (236°C), 542 K (269°C), and 565 K (292°C), respectively, show that the amount of η phase intermetallics increased considerably with increasing temperature. Figure 7a–d, which depicts the microstructural evolution in samples reflowed at 565 K (292°C) for times of 0.67 min, 1.5 min, 4.0 min, and 8.0 min, shows the amount of η phase intermetallics present to increase with time. The results of quantitative metallographic measurements of the volume fractions of primary β(Sn) dendrites, eutectic and η phase intermetallic are plotted in Figs. 8, 9, and 10, respectively. From these figures it can be seen that the volume percent of β(Sn) dendrites and η phase intermetallics increase with increasing reflow temperature and reflow time, while the interdendritic eutectic decreases. These microstructural changes can be explained on the basis of the increase in Cu dissolution into the molten solder with increasing temperature (Figs. 1 and 2) and time (Fig. 2).

As can be seen in Fig. 1, higher temperatures result in a higher solubility limit and, hence, a greater amount of dissolved Cu at saturation. As can be seen

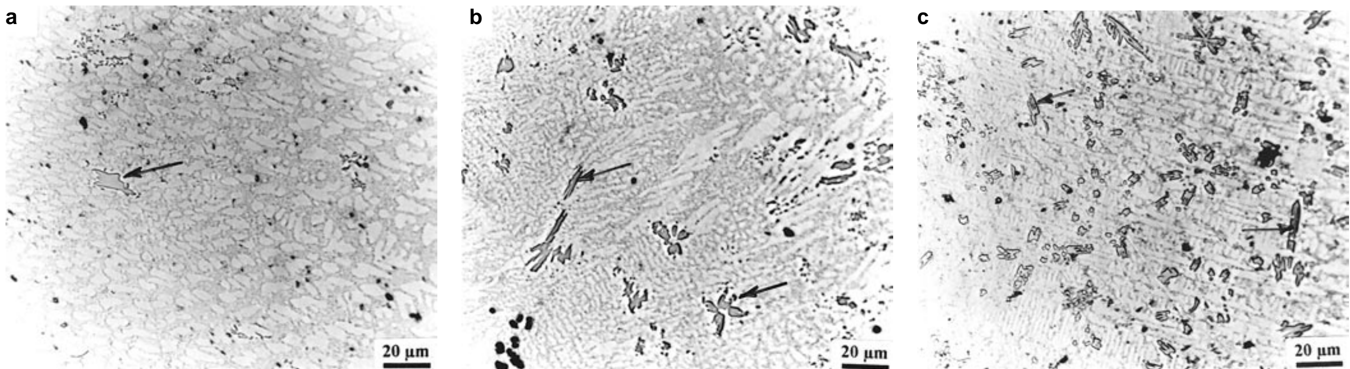

Fig. 6. Micrographs from samples isothermally reflowed for 60 sec at (a) 509 K (236°C), (b) 542 K (269°C), and (c) 565 K (292°C) showing the increase in η phase intermetallics (arrows) with increasing temperature.

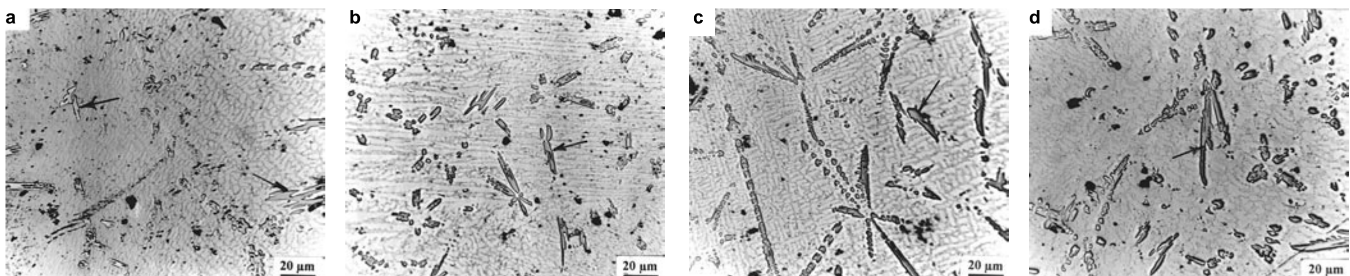

Fig. 7. Micrographs from samples reflowed at 565 K (292°C) for times of (a) 0.67 min, (b) 1.5 min, (c) 4.0 min, and (d) 8.0 min showing the increase in η phase intermetallics (arrows) with increasing time.

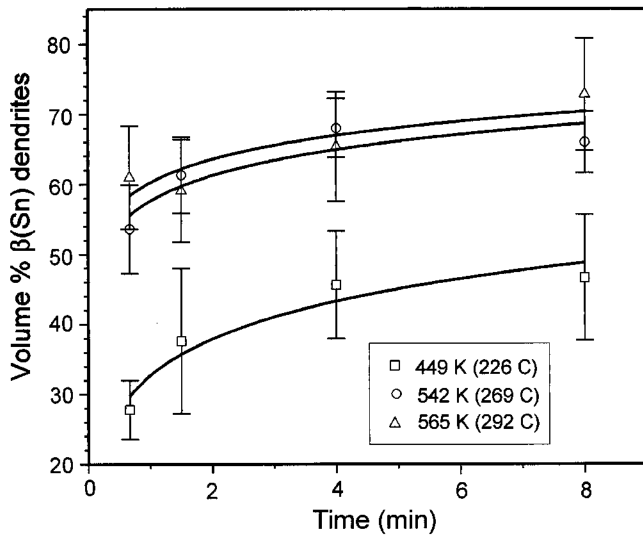

Fig. 8. Volume percent of β(Sn) dendrites versus reflow time.

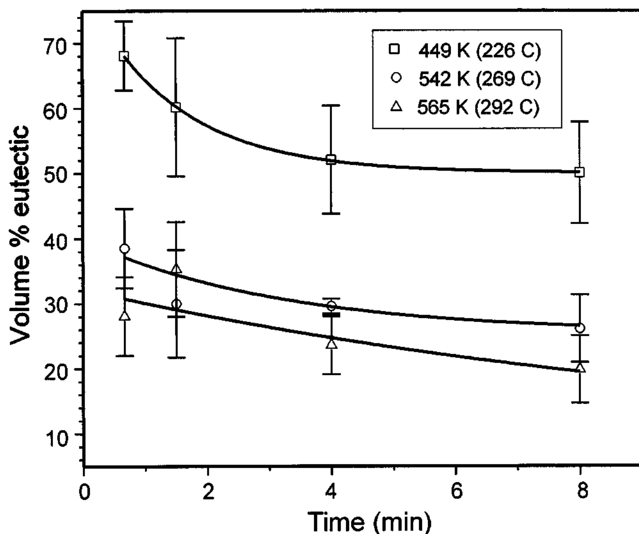

Fig. 9. Volume percent of eutectic versus reflow time.

in Fig. 2 the amount of Cu dissolved at temperatures ranging from 527 K (254°C) to 575 K (302°C) increases rapidly for At/V values up to about 10 and then levels off as if saturation has been achieved. Considering that A/V values for the specimens used to determine the data in Fig. 2 are on the order of 3 mm^2/mm^3, the initial rapid increase in Cu content occurs in the first 2 min of reflow. This corresponds to the initially rapid volume fraction changes in β(Sn) dendrites and eutectic in Figs. 8 and 9, which occur in the first 4 min of reflow. Of the above described microstructural changes, two observations must be explained. First, reasons for the increase in the volume fraction of β(Sn) dendrites and the consequent decrease in the amount of eutectic must be given. Second, an explanation for the increase in the volume fraction of η phase intermetallic must be proposed. With respect to the increase in the volume fraction of β(Sn) dendrites, experimental evidence (not shown) shows that their presence is partly the result of non-

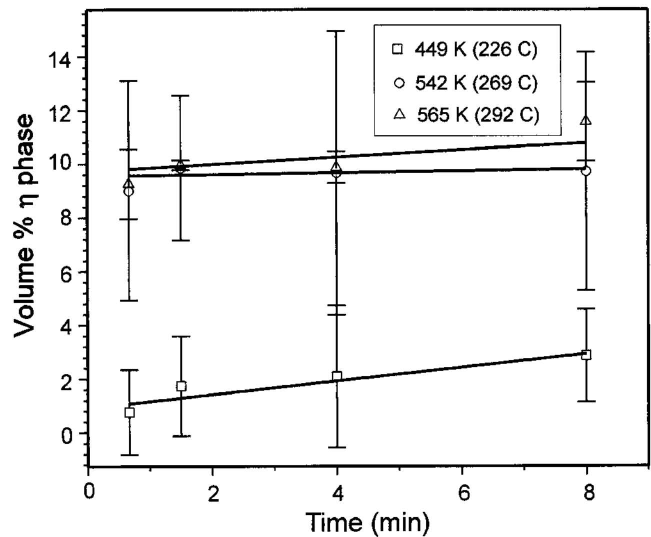

Fig. 10. Volume percent of η phase intermetallic versus reflow time.

equilibrium solidification effects. According to the binary Sn-Ag phase diagram the binary Sn-3.8at.%Ag solder alloy has the eutectic composition and, as such, should exhibit no primary β(Sn) dendrites in its as solidified microstructure; however, examination of the microstructure of the pure binary alloy solidified under even slow cooling conditions reveals their presence. This suggests that the alloy supercools to some temperature below the eutectic before eutectic solidification begins and that this is accompanied by a shift of the eutectic composition to a higher Sn content. This would allow primary β(Sn) dendrites to form prior to eutectic solidification. While this displacement of the eutectic transformation to lower temperatures can explain the presence of β(Sn) dendrites, it cannot explain why their volume percent would increase with increasing Cu content. This requires knowledge of the Ag-Cu-Sn phase diagram. Since the relevant isotherms and vertical sections of the diagram have not been published, they are constructed here using existing binary and ternary phase equilibrium data.

Using the binary Sn-Ag phase diagram, the Cu-Sn phase diagram, published data on the β(Sn), η, ε″(Ag_3Sn), L ternary reactions in the Ag-Cu-Sn system[4,5] and published work[6] on the β(Sn), η, ε″ phase equilibrium at 310 K (37°C), the various parts of the Ag-Cu-Sn phase diagram shown in Figs. 11, 12, 13, and 14 were constructed. The ternary eutectic reaction,

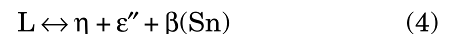

$$L \leftrightarrow \eta + \varepsilon'' + \beta(Sn) \quad (4)$$

reported by Miller et al. to occur at 490 K (217°C) and an alloy composition Sn-5.1Ag-3.1Cu by at.% are shown as the tie triangle in Fig. 11. An enlarged view of the Sn rich corner of this triangle is shown in Fig. 12. As can be seen in the figures, the eutectic E lies at the end of three monovariant reaction curves indicated by lines e_1E, e_2E, and TE descending from higher temperatures. The monovariant three-phase equilibrium,

$$L \leftrightarrow \eta + \beta(Sn) \quad (5)$$

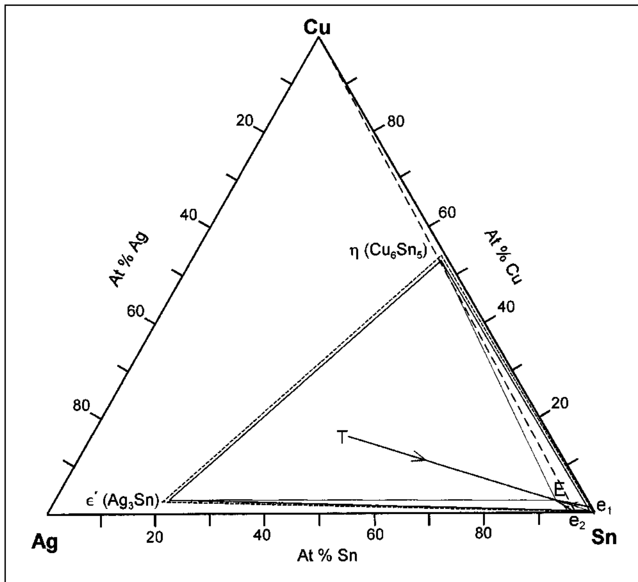

Fig. 11. Ag-Sn-Cu ternary phase diagram showing the β-Sn, η, ε″, L tie triangles at the ternary eutectic temperature of 490 K (217°C) (light solid lines), the β(Sn), η, ε″ tie triangle at 310 K (37°C) (light dashed line), the ternary eutectic E at 490 K (217°C), the binary Cu-Sn eutectic e_1 at 500 K (227°C), the binary Ag-Sn eutectic e_2 at 494 K (221°C), the ternary reaction T, the projections of the monovariant reactions extending from e_1, e_2, and T to the ternary eutectic E (solid lines), and the line followed when Cu is added to Sn-3.8at.%Ag alloy (heavy dashed line).

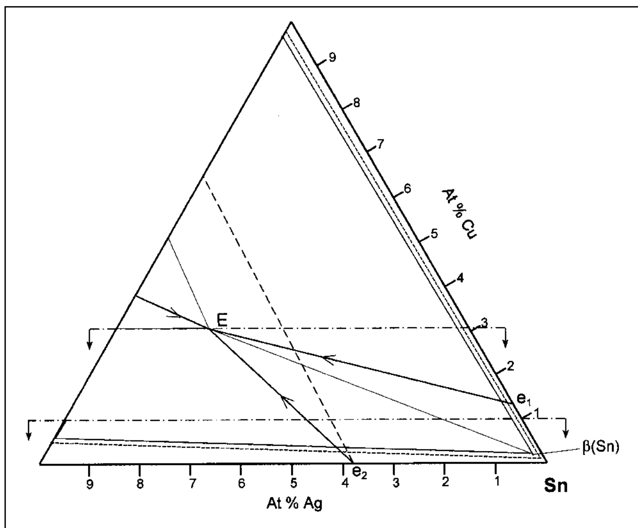

Fig. 12. Enlarged view of the Sn rich corner of Figure 11. The horizontal lines represent constant Cu compositions of 1.0 at.%Cu and 3.1 at.%Cu.

originates at the binary Cu-Sn eutectic e_1 at 500 K (227°C). The monovariant three-phase equilibrium,

$$L \leftrightarrow \varepsilon'' + \beta(Sn) \quad (6)$$

begins at the Ag-Sn binary eutectic e_2 at 494 K (221°C). The equilibrium,

$$L \leftrightarrow \eta + \varepsilon \quad (7)$$

evolves from another ternary reaction T. E represents the invariant ternary eutectic point at 490 K (217°C).

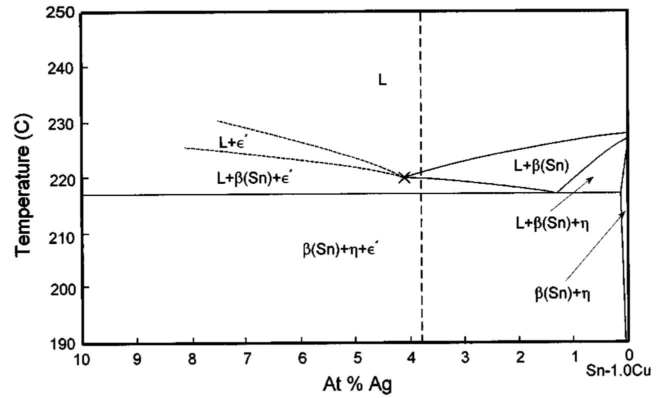

Fig. 13. Vertical section through the Sn-Ag-Cu ternary system at a constant Cu concentration of 1.0 at.%.

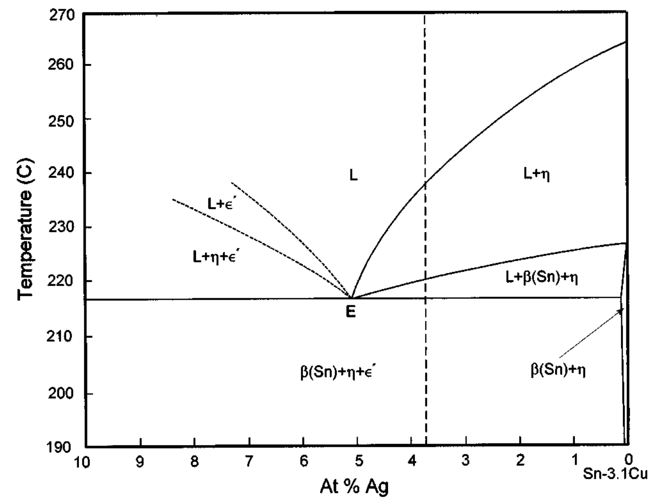

Fig. 14. Vertical section through the Sn-Ag-Cu ternary system at a constant Cu concentration of 3.1 at.%.

For alloys falling within the β(Sn), η, ε″ tie triangle, three-phase equilibrium between β(Sn), η, and ε″ exists from just below 490 K (217°C) to room temperature, where the phase equilibrium is described by the light dashed line tie triangle.[6]

The heavy dashed line beginning at e_2 in Figs. 11 and 12 is the composition followed by Sn-3.8at.%Ag solder when Cu is dissolved in it, and the section lines in Fig. 12 represent constant Cu concentrations of 1.0 and 3.1 at.%Cu. Two possible vertical sections corresponding to constant Cu concentration values of 1.0 at.%Cu and 3.1 at.%Cu consistent with the Sn-Ag and Cu-Sn binary diagrams and the ternary diagram (Figs. 11 and 12) are given in Figs 13 and 14. The vertical dashed lines in these figures represent the composition of a binary eutectic Sn-Ag solder after the amount of Cu associated with the vertical sections has been added to the solder. Hence, the vertical sections can be used to predict what phases might be formed in solder as the result of Cu dissolution. In both vertical sections, the intersection with the four-phase field (invariant ternary eutectic) is indicated by the horizontal line at 490 K (217°C), and in the vertical section in Fig. 13 the intersection with the monovariant reaction originating at e_2 is indicated by an X.

Table I. Summary of Experimentally Measured and Numerically Predicted Cu Contents of Sn-3.8at.%Ag Solder for Six Different Non-Isothermal Reflow Conditions

Specimen Number	Reflow Method	T_M (K)	T_P (K)	T_S (K)	R_H (K/min)	R_C (K/min)	t_R (min)	At.%Cu Dissolved	
								Measured	Predicted
1	Programable	491	513	476	5.6	4.4	13.8	2.03 ± 0.53	2.53
2	Oven	492	536	477	5.6	4.8	21.7	2.74 ± 0.46	3.58
3		491	514	475	5.6	39.8	5.0	1.58 ± 0.31	2.51
4		492	535	475	5.6	37.9	10.4	2.13 ± 0.69	3.51
5	Hot Plate, Cu Block Quench	493	514	483	5.6	620	3.1	2.49 ± 0.32	2.44
6		490	534	477	5.6	1210	8.5	3.33 ± 0.73	3.38

T_M=melting temperature, T_P=peak temperature, T_S=solidification temperature, R_H=average heating rate, R_C=average cooling rate, t_R=total reflow time

With respect to microstructural development, the vertical sections at 1.0 at.%Cu and 3.1 at.%Cu show that Cu dissolution into an eutectic Sn-Ag alloy should lead to the formation of primary β(Sn) dendrites, even without the non-equilibrium cooling effect mentioned previously. Further, the vertical sections show that as Cu content increases the amount of primary β(Sn) should increase.

The ternary diagrams in Figs. 11 and 12 show that, even for low Cu concentrations, a ternary eutectic reaction should occur during cooling, resulting in a three-phase mixture. In the present study the interdendritic mixture is too fine to determine if this reaction occurs.

Figure 14 predicts the formation of primary η(Cu_6Sn_5) intermetallics prior to the formation of β(Sn) dendrites, when the Cu concentration in the molten solder is 3.1 at.%Cu. Figure 12 indicates that one should start to get these dendrites when the Cu concentration reaches 2.6 at.%Cu. The presence of η intermetallics in the bulk solder (Figs. 6 and 7), presumably from primary crystallization, suggests that the Cu concentration at some places of the solder is greater than 2.6 at.%Cu. Their presence even after short reflow times may result from the apparently directional solidification of the solder in Fig. 5. Solidification apparently began at the Cu substrate and progressed to the solder surface. Conceivably, the molten solder ahead of the solid-liquid interface could become enriched in Cu to the point at which primary η phase could form.

As a final note it should be pointed out that a recent study by Loomans and Fine[7] indicates that the ternary eutectic is at Sn-3.8at.%Ag-1.7at.%Cu rather than at the value reported by Miller, Anderson and Smith.[4] While using this value would, of course, change the phase diagrams presented here, it would not alter the conclusions drawn.

Numerical Method for Predicting the Amount of Cu Picked Up by Solder under Non-Isothermal Conditions

The amount of Cu substrate picked up by solder through dissolution under non-isothermal reflow conditions can be predicted using a numerical method similar to that developed for the prediction of intermetallic layer growth between molten solder and a substrate.[8,9] The method requires as input the temperature-time profile for the solder while it is molten and in contact with the Cu, the solubility parameters X^{S0} and Q_S in Eq. 1, the parameters K^0 and Q_d required to calculate the constant K in the Nernst-Brunner equation (Eq. 2), the solder/substrate surface area (A), the solder volume (V), and the initial concentration (X^0) of Cu in the solder. Basically, the method involves dividing up the period of the soldering process from the time at which the solder melts on the substrate to the time at which it solidifies into n equal time intervals Δt and then, starting with the first interval after melting, calculating the amount of solute dissolved in each interval using the Nernst-Brunner equation until saturation is reached.

The temperatures (T_i), times (t_i), Cu concentrations (X_i), etc. associated with any given time interval are identified with a subscript i. Thus, the ith interval has an average temperature,

$$\overline{T}_i = \frac{T_i - T_{i-1}}{2} \tag{8}$$

where T_i is the temperature at the end of the ith interval and T_{i-1} is the temperature at the start of it. The Cu concentration X_i at the end of the ith interval can be calculated using the Nernst-Brunner equation adapted for this interval:

$$\ln \frac{X_i^S - X_{i-1}}{X_i^S - X_i} = \frac{K_i A \Delta t}{V} \tag{9}$$

Here X_{i-1} is the Cu concentration in the solder calculated by the previous calculation for the i-1th interval. K_i is given by

$$K_i = K^0 \exp\left(-\frac{Q_d}{R\overline{T}_i}\right) \tag{10}$$

and X_i^S is given by

$$X_i^S = X^{S0} \exp\left(-\frac{Q_S}{R\overline{T}_i}\right) \tag{11}$$

Thus, to calculate the Cu concentration after any particular interval one uses Eqs. 8–11 to calculate the concentration X_1 at the end of the first interval. Then, using this value of X_1 one calculates X_2 and so on until $X_I = X_i^S$.

Table I shows predictions of the amounts of Cu picked up during non-isothermal reflow soldering experiments using the above method along with the measured values of the Cu concentrations in the solder of the specimens. The reflow conditions given in Table I for these non-isothermal experiments are the same as those reported previously for growth of intermetallic layers under non-isothermal conditions.[9] These non-isothermal conditions involved heating the solder on a Cu substrate at a constant rate (R_H) to a peak temperature (T_P) and then cooling it at a constant rate (R_C) until the solder solidified. Values of the melting temperature (T_M), the solidification temperature (T_S), and the total soldering time (t_R) were obtained from a thermocouple imbedded in solder on a dummy specimen subject to the same reflow.

The calculations were performed with a FORTRAN program based on the above numerical method. The program required as input the values of the solubility parameters, X^{S0} and Q_S, and the Nernst-Brunner parameters, K^0 and Q_d, given in Figs. 1 and 3, respectively. It also required the temperature profile parameters (T_M, T_P, R_H, R_C and t_R) given in Table I and the number of intervals n, into which the soldering time t_R was divided up into. This was taken to be 100,000.

From Table I it can be seen that the predicted values agree very well with the experimentally measured Cu concentration values for the fastest cooling rate studied. However, the predicted values are higher than the experimental values for the slower cooling rates. The discrepancy between the measured and calculated values could result from reprecipitation of dissolved Cu during the cooling part of the temperature-time profile for the reflow experiments with slower cooling rates. This possible reprecipitation after saturation is reached during cooling is not taken into account in the numerical calculation, as the calculation stops when saturation is reached.

ACKNOWLEDGEMENTS

The authors gratefully acknowledge Visteon Automotive Systems for supporting this work. Also, one of the authors, W. Laub, wishes to express his gratitude to the Alexander von Humboldt Foundation for their support during the course of the study.

REFERENCES

1. R.J. Klein Wassink, *Soldering in Electronics,* 2nd ed. (Ayr, Scotland: Electrochemical Publications Ltd., 1989), pp. 141–185.
2. M. Schaefer, W. Laub, R.A. Fournelle, and J. Liang, *Design and Reliability of Solders and Solder Interconnects*, ed. R.K. Mahidhara et al. (Warrendale, PA: TMS, 1997), p. 247.
3. *ASM Handbook, 10th Ed., Vol. 3, Alloy Phase Diagrams*, (Materials Park, OH: ASM Int., 1992), p. 178.
4. C.M. Miller, I.E. Anderson, and J.F. Smith, *J. Electron. Mater.* 23, 595 (1994).
5. C.M. Miller, "Development of a New Pb-Free Solder: Sn-Ag-Cu," Master of Science Thesis, Iowa State University, Ames, IA, 1994.
6. P. Villars, A. Prince, and H. Okamoto, *Handbook of Ternary Alloy Phase Diagrams: Vol. 3* (Materials Park, OH: ASM Int., 1995).
7. M.E. Loomans and M.E. Fine, *Metall. Trans. A* 31A,1155 (2000).
8. M. Schaefer, W. Laub, J.M. Sabee, and R.A. Fournelle, *J. Electron. Mater.* 25, 992 (1996).
9. S. Chada, W. Laub, R.A. Fournelle, and D. Shangguan, *J. Electron. Mater.* 28,1194 (1999).